

Numerical Analysis of Indoor MIMO-SDM Transmission Using Antenna Selection Diversity

Kazuki SAITO , Qiang CHEN and Kunio SAWAYA
 Graduate School of Engineering, Tohoku University
 6-6-05 Aramaki Aza Aoba, Aoba-ku, Sendai, 980-8579 Japan
 Email: {saitok, chenq, sawaya}@tohoku.ecei.ac.jp

Abstract—Channel capacity of indoor Multi-input Multi-output Space Division Multiplexing (MIMO-SDM) with antenna selection diversity is analyzed using the ray tracing method. A large number of receiving antennas are divided into several blocks. Each block is corresponding to a receiving MIMO channel, and the number of transmitting channel is assumed to be equal to the number of receiving channel. The number of divided blocks is changed and the channel capacity is evaluated in many antenna locations. It is found that, in the case of a weak fading environment, decreasing the number of divided blocks can improve the channel capacity per channel. On the other hand, increasing the number of blocks can lead to increase the channel capacity per channel in the case of a rich fading environment.

I. INTRODUCTION

Because of the strong requirement of high speed data transmission service, many techniques of wideband mobile communications have been studied. The multiple input multiple outputs (MIMO) multiplexing is an attractive technique to achieve very high speed transmission with a limited bandwidth[1]-[3]. The frequency utilization efficiency can be greatly improved when the MIMO-Space Division Multiplexing (SDM) technology is used in wireless communication systems.

The millimeter wave band has attracted great interest for its wide bandwidth allocated for future broadband wireless communications[4],[5]. Therefore, a combination of MIMO technique and millimeter wave band can be used to realize an ultra high-speed wireless communications.

A large number of receiving antennas for MIMO can be easily implemented in a mobile handset by using the advantage of the millimeter wave because miniaturization of the antenna size is possible in the millimeter wave band. The large number of antennas can be divided into several groups. The selection diversity processing can be performed inside each group, and each group can be used as one of the channels in the MIMO-SDM. Combination of MIMO-SDM and antenna selection diversity has been studied theoretically[6]-[8].

In this study, propagation characteristics of MIMO-SDM with antenna selection diversity in indoor environment at millimeter wave band are numerically analyzed. The effect of the number of antenna blocks, antenna elements in each blocks and the number of total antennas on MIMO transmission capacity is investigated to show how to optimize the group size to obtain the high MIMO transmission capacity.

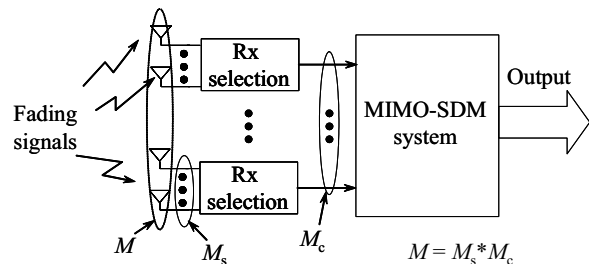


Fig. 1. Receiving system of MIMO-SDM with antenna selection diversity.

TABLE I
ANALYSIS SPECIFICATION.

Frequency	60 GHz ($\lambda_0 = 5$ mm)
Transmission antenna	Omnidirectional antennas
Receiving antenna	Dipole antennas
Antenna spacing	$0.5\lambda_0$
Transmission power	0 dBm
Received noise level	-100 dBm

II. MIMO-SDM TRANSMISSION USING ANTENNA SELECTION DIVERSITY

A. Receiving system

Receiving system is shown in Fig. 1. M is the number of total receiving antennas. M_s is the number of antenna elements in each group which process selection diversity. M_c is the number of groups. Thus $M = M_s * M_c$.

Received signal was processed in the way of selection antenna diversity which select a maximum receiving SNR in M_s elements in one block. The selected M_c signals are used as the input signal in the MIMO-SDM receiving system. In this study, the MIMO channel capacity was calculated by changing the number of total receiving antennas M and the number of block M_c .

B. MIMO Channel Capacity

Propagation channel between transmitting and receiving antennas can be calculated by numerical analysis. The channel transmission matrix \mathbf{H} is obtained from the propagation channel as shown in the following equation.

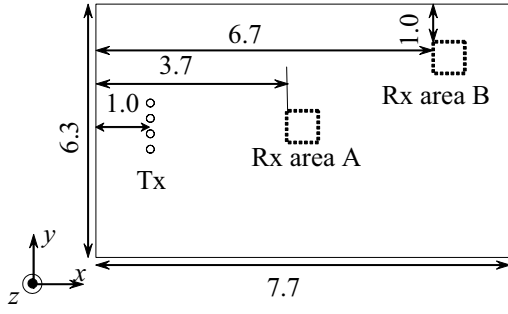


Fig. 2. Indoor model (Unit:m).

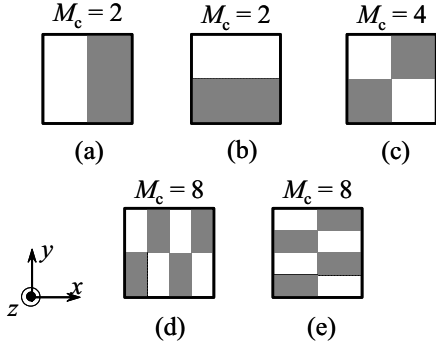


Fig. 3. Pattern of receiving antennas.

$$g_{ij} = \sum_{k=1}^K P_{ij}(k), \quad i = 1, 2 \dots N_r, \quad j = 1, 2 \dots N_t \quad (1)$$

where N_t is number of transmitting antenna, N_r is number of receiving antenna, K is number of path which reach receiving antenna from transmission antenna. g_{ij} is element of channel matrix \mathbf{G} which is calculated by ray tracing. $P_{ij}(k)$ is channel response of the ray which reaches the i -th receiving antenna through the k -th propagation channel from the j -th transmitting antenna.

It is known that MIMO channel capacity is calculated by channel transmission matrix which is normalized by the received power shown in the following.

$$\mathbf{H} = \mathbf{A}\mathbf{G} \quad (2)$$

$$\mathbf{A} = \left(\sum_{i=1}^{N_r} \sum_{j=1}^{N_t} E[|g_{ij}|^2] / N_t N_r \right)^{-\frac{1}{2}} \quad (3)$$

where $E[\cdot]$ is ensemble average. The MIMO channel capacity is calculated by [9],

$$C = \sum_{j=1}^{N_t} \log_2(\lambda_j \gamma_0 / N_t + 1) \quad [\text{bit/s/Hz}] \quad (4)$$

where $N_t \leq N_r$, λ_j is eigenvalue of $\mathbf{H}^H \mathbf{H}$, γ_0 is average received SNR.

C. Simulation method

The method of moments and the FDTD (Finite Difference Time Domain) method are known well to analyze the field distribution around scatterer. A high accurate analysis is possible by using these methods. On the other hand, it takes very large memory and long calculation time when the size of scatterers and antennas, and propagation path length are much larger than wavelength. However, the ray tracing method, which is a kind of high-frequency approximation methods, is an efficient method in calculating the electrically large scale problems. Therefore, the ray tracing method is applied to the numerical analysis of propagation channel in the present study[10].

Either a ray launching method or an image method is required in the ray tracing method. The ray launching method follows up many ray's propagation path which generated from transmitting antennas, while the image method calculate reflection path from scatterer using image path. The ray launching method is more suitable than the imaging method in saving CPU time when a large amount of scatterers are included in the analysis model, although the image method usually gives results with a higher accuracy. However, phase information of each receiving paths is very important when calculating MIMO channel capacity. Therefore, an accurate path length should be estimated more accurately to obtain a higher accurate MIMO channel capacity. As a result, the image method is used in this study.

Analysis specification is shown in Tab. I. Frequency is 60 GHz. Antenna element spacing is $0.5 \lambda_0 = 2.5\text{mm}$. The total transmission power is 0 dBm. Received noise level is defined as -100 dBm. In the imaging method, the maximum number of reflection times is assumed to be 3. No diffraction wave is considered in the analysis.

III. ANALYSIS MODEL

This section describes the indoor model and antenna geometry in the simulation. The indoor model is a rectangular room bounded by a concrete wall ($\epsilon_r = 6.765, \sigma = 2.3 \times 10^{-3} \text{ S/m}$) with 10 cm thickness as shown in Fig. 2. The room has a length of 7.7 m, width of 6.3 m, and height of 2.5 m. Center of transmitting antenna arrays are located at (1.0 m, 3.15 m) at a height of 1.5 m. Receiving antennas are placed at 2 positions, i.e., area A and area B, at a height of 1.5 m.

The transmitting antenna is assumed to have an isotropic radiation pattern. The receiving antennas have several types of geometries: $M = 24 * 24, 16 * 16, 8 * 8$ and $4 * 4$. The receiving antennas are divided into several blocks which is shown in Fig. 3. The divided patterns of antennas are named as (a), (b), (c), (d), (e), respectively. MIMO channel capacity was calculated. Radiation pattern of receiving antenna is unidirectional. Antenna has a gain of 4.53 dBi and has a vertical polarization.

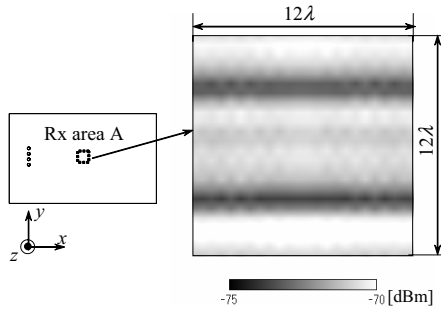


Fig. 4. Received power distribution of receiving antennas at area A ($M = 24 * 24$).

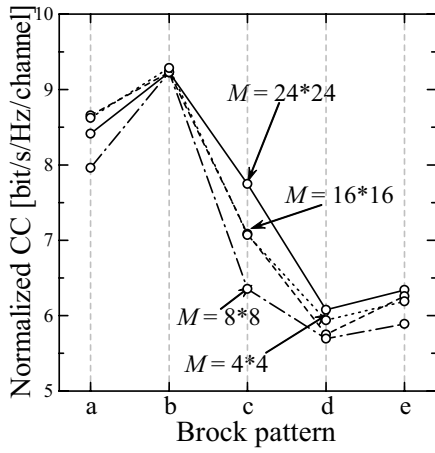


Fig. 5. Normalized MIMO channel capacity at area A.

IV. SIMULATION RESULTS

A. Simulation results in area A

The spatial distribution of received power in area A is shown in Fig. 4.

Antenna selection diversity was applied to the received signal inside each antenna group. First, received power at each receiving antenna was calculated by using the ray tracing method. Then, the antenna element was selected which has the maximum SNR in each group which is shown in Fig. 3. The selected antenna element was used as one of the MIMO-SDM branches. The number of transmitting antennas is assumed to be equal to the number of blocks M_c of receiving antennas. The MIMO channel capacity was evaluated by changing the total number of receiving antennas M and the number of divided blocks M_c . The MIMO channel capacity was normalized by the number of MIMO branches, i.e. the number of blocks of the receiving antennas. The MIMO channel capacity was calculated for every movement of the receiving antennas in direction x at a step of $0.1\lambda_0$ and then was averaged at areas of A and B, respectively.

Normalized MIMO channel capacity is shown in Fig. 5. It is found that decreasing the number of divided blocks can improve the normalized channel capacity.

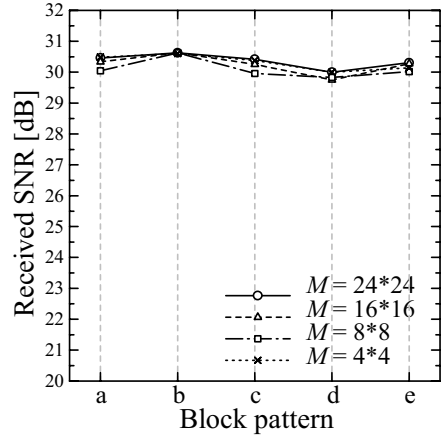


Fig. 6. Average received SNR at area A.

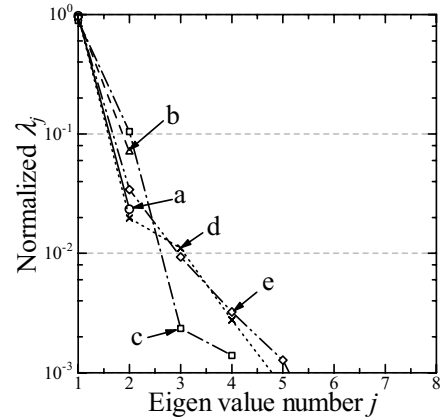


Fig. 7. Normalized eigen value at area A.

Average of received SNR (signal to noise power ratio) of the output of selection diversity is shown in Fig. 4. Only 0.5 dB improvement is observed by using the selection diversity because of the weak fading environment as shown in Fig. 4. Therefore, effect of the antenna selection diversity is very limited.

The normalized eigenvalues are shown in Fig. 7. It is found that the normalized eigenvalues of more than 3 order becomes very small because of the level of the reflection paths is very small due to the large propagation loss at the millimeter wave band in the case of $M_c = 4$ (c) and $M_c = 8$ (d,e). Therefore, normalized MIMO channel capacity per channel becomes small than that at $M_c = 2$.

B. Simulation result in area B

The spatial distribution of received power in area B is shown in Fig. 8. It is found that a strong fading environment is observed in area B. The normalized MIMO channel capacity is shown in Fig. 9. When the number of divided blocks M_s increases, the normalized channel capacity per channel does not decrease as rapidly as that in the case of area A.

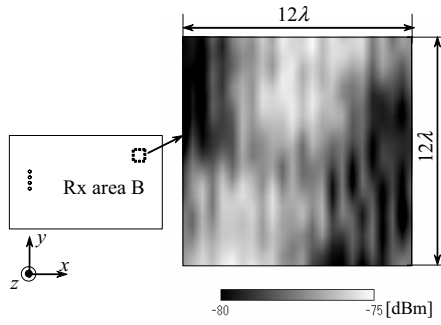


Fig. 8. Received power distribution of receiving antennas at area B ($M = 24 * 24$).

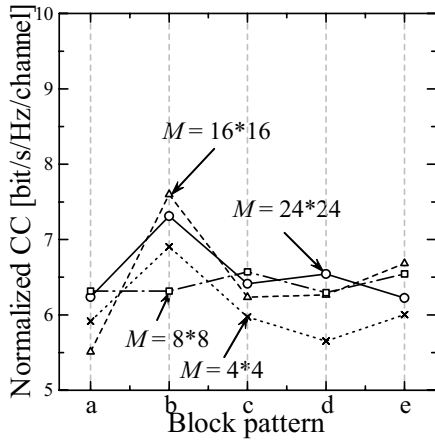


Fig. 9. Normalized MIMO channel capacity at area B.

The average of received SNR of the output of selection diversity is shown in Fig. 10. This result is different from that in the case of area A. A strong correlation is observed between the number of antenna elements M_s in each divided block and the received SNR as shown in Fig. 11. A 5-dB difference appears in the averaged received SNR for various numbers of M_s .

However, the normalized channel capacity per channel does not change as much as the SNR when M_s changes. The eigenvalues are shown in Fig. 12. The normalized eigenvalues are larger than that in the case of area A because the reflection paths from walls cause a strong fading in area B as shown in Fig. 8. From these results, a high received SNR can be obtained by increasing the number of elements M_s in each divided block, which contributes to increase the MIMO channel capacity per channel.

V. CONCLUSION

In this study, MIMO-SDM with antenna selection diversity was investigated. Indoor propagation characteristics at millimeter band was analyzed by using the ray tracing method. Effect of the number of receiving antennas, number of divided blocks for selection diversity on the normalized MIMO-SDM

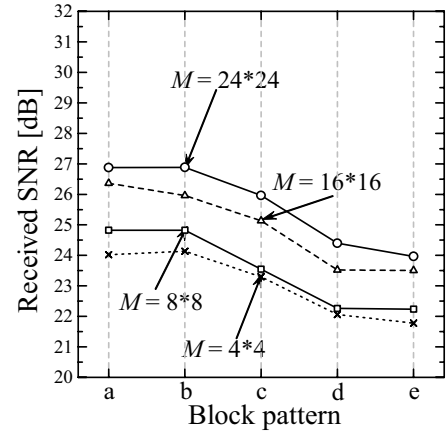


Fig. 10. Average received SNR at area B.

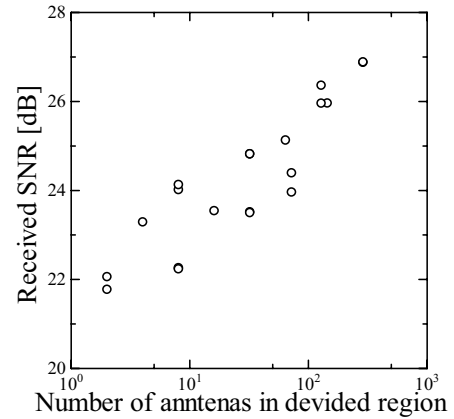


Fig. 11. Number of elements in each divided block M_s and received SNR.

channel capacity was obtained. In the case of weak fading environment, because a high performance of MIMO-SDM can not be expected, the normalized channel capacity per channel can be increased by decreasing the number of divided blocks. On the other hand, in the case of strong fading environment, although the effect of the antenna selection diversity can improve the SNR, a large number of divided blocks can result in a high channel capacity due to the rich reflection paths.

REFERENCES

- [1] G. J. Foschini and M. J. Gans, "On Limits of Wireless Communications in a Fading Environment when Using Multiple Antennas," *Wireless Personal Communications* 6, pp. 311-335, 1998.
- [2] T. Ohgane, T. Nishimura and Y. Ogawa, "Applications of Space Division Multiplexing and Those Performance in a MIMO Channel," *IEICE Trans. Commun.*, vol.J87-B, No. 9, pp. 1162-1173, Sept. 2004.
- [3] Y. Karasawa, "MIMO Propagation Channel Modeling," *IEICE Trans. Commun.*, vol.J86-B, No.9, pp.1706-1720, Sept. 2003.
- [4] Nan Guo, Robert C. Qiu, Shaomin S. Mo, and Kazukai Takahashi, "60-GHz Millimeter-Wave Radio: Principle, Technology, and New Results," *EURASIP Journal on Wireless Communications and Networking*, Vol. 2007, Article ID 68253.
- [5] T. Ohno and K. Ogawa, "A Sector Array Using Dielectric Loaded Antennas for Indoor High-Speed Wireless LAN Applications at 60GHz," *IEICE Trans. Commun.*, vol.J88-B, No.9, pp. 1738-1751, Sept. 2005.

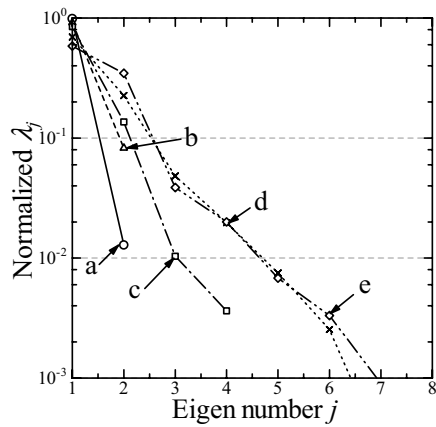


Fig. 12. Normalized eigen values at area B.

- [6] S. Sanayei and A. Nosratinia, "Antenna selection in MIMO systems," IEEE communications Magazine, pp. 68-73, October 2004.
- [7] M. K. Simon and M. Alouini, "A compact performance analysis of generalized selection combining with independent but, nonidentically distributed Rayleigh fading paths," IEEE Trans. Commun., vol. 50, no. 9, pp. 1409-1412, September 2002.
- [8] R. K. Mallik and M. Z. Win, "Analysis of hybrid selection/maximal-ratio combining in correlated Nakagami fading," IEEE Trans. Commun., vol. 50, no. 8, pp. 1372-1383, August 2002.
- [9] E. Telatar, "Capacity of multi-antenna gaussian channels," European transactions on Telecommunications, vol.10, no. 6, pp. 585-595, Nov./Dec. 1999.
- [10] C.-P. Lim, M. Lee, R. J. Burkholder, J. L. Volakis, and R. J. Marhefka, "60 GHz Indoor Propagation Studies for Wireless Communications Based on a Ray-Tracing Method," EURASIP Journal on Wireless Communications and Networking, Vol. 2007, Article ID 73928.